

Efficient Analytical Derivatives of Rigid-Body Dynamics using Spatial Vector Algebra

Shubham Singh¹, Ryan P. Russell² and Patrick M. Wensing³

Abstract—Optimization algorithms are increasingly important for the control of rigid-body systems. An essential requirement for these algorithms is the availability of accurate partial derivatives of the equations of motion with respect to the state and control variables. State of the art methods for calculating the derivatives use analytical differentiation methods based on the chain rule, and although these methods are an improvement over finite-difference in terms of accuracy, they are not always the most efficient. In this paper, we present an analytical method for calculating the first-order partial derivatives of rigid-body dynamics. The method uses Featherstone’s spatial vector algebra and is presented in a recursive form similar to the Recursive-Newton Euler Algorithm (RNEA). Several dynamics identities and computational options are exploited for efficiency. The algorithms are benchmarked against competing approaches in Fortran and C++. Timing results are presented for kinematic trees with up to 500 links. As an example, the 100 link case leads to a $7\times$ speedup over our Fortran implementation of the existing state-of-the-art method. Preliminary comparison of compute timings for the partial derivatives of inverse dynamics in C++ are also shown versus the existing Pinocchio framework. A speedup of $1.6\times$ is reported for the 36-dof ATLAS humanoid using the new algorithm proposed in this paper.

I. INTRODUCTION

Rigid-body dynamics are widely used in the development of control algorithms for quadruped and humanoid robots, with recursive rigid-body dynamics algorithms at the heart of many modern real-time controllers. The most common current approaches for controller design of legged robotics rely on optimization and optimal control theory [1], [2]. Popular robotics libraries like Crocodyl [3] and Drake [4] heavily depend on optimization algorithms that require the partial derivatives of the rigid-body dynamics with respect to the state and control variables. The calculation of these derivatives accounts for the majority of CPU time required for many optimal control applications [6]. One common approach for calculating the derivatives of rigid-body dynamics uses finite difference formulas [5], [7], [8]. These methods are simple to implement, are often computed in parallel,

but suffer in accuracy (Table I). Another common approach used for calculating partial derivatives is automatic differentiation (Auto-diff), also called "algorithmic differentiation" [4], [9], [10]. Auto-diff automatically calculates the partials of an algorithm using operator overloading [9] or source code transformation [4], [10]. The first approach overloads basic data types to compute partials concurrently with all arithmetic. The second approach builds an expression graph and alters source code to calculate the partial derivatives. The complex-step method [11] works by perturbing one state at a time in the complex dimension. The complex-step approach is accurate to machine precision but requires all functions to be computed in the complex plane and requires more computation than Auto-diff (Table I). Cossette et al. [12] showed its use to obtain Jacobians of functions that have matrix Lie group elements as arguments, indicating potential use in rigid-body dynamics.

While rigid-body-dynamics algorithms based on chain-rule expressions lead to general purpose algorithms, special-purpose algorithms can further exploit the specific structure in the complex rigid-body equations of motion. One such approach is the Lagrangian method (Lag-diff) based on Lie group/algebra to calculate the partial derivatives of rigid-body dynamics. An example is presented in Ref. [13], where partial derivatives are computed of the mass matrix $M(\mathbf{q})$, the Coriolis matrix $C(\mathbf{q}, \dot{\mathbf{q}})$, and the gravity vector $\mathbf{g}(\mathbf{q})$ with respect to the state variables \mathbf{q} and $\dot{\mathbf{q}}$, leading to an $\mathcal{O}(N^3)$ algorithm, where N is the number of links in the system.

Ref. [14] shows another $\mathcal{O}(N^2)$ analytical method for partial derivatives of inverse and forward dynamics for serial kinematic trees.

Analytical chain-rule differentiation, which uses the manually computed chain-rule of an algorithm, is another method used to calculate partial derivatives of rigid-body dynamics. Ref. [6] applies this approach on the inverse dynamics algorithm. Although the resulting inverse dynamics partials algorithm is of order $\mathcal{O}(Nd)$ (where d is the depth of the kinematic tree), the forward dynamics partials algorithm scales as $\mathcal{O}(N^3)$.

In this work, we first independently derive the expressions for partial derivatives of inverse dynamics, earlier shown in Ref. [14], with a new emphasis on general branched kinematic trees. We formulate the analytical

¹Graduate Research Assistant, Aerospace Engineering, The University of Texas at Austin, TX-78751, USA. singh281@utexas.edu

²Associate Professor, Aerospace Engineering, The University of Texas at Austin, TX-78751, USA. ryan.russell@utexas.edu

³Assistant Professor, Aerospace & Mechanical Engineering, University of Notre Dame, IN-46556, USA. pwensing@nd.edu

Method	Abbreviation	Implementation (Easy/Medium/Hard)	Speed (Slow/Medium/Fast)	Accuracy (Low/Medium/High)
Finite difference [5], [7], [8]	Num-diff	Easy	Medium	Low
Complex-step Differentiation [12]	Complex-step	Easy	Slow/Medium	High
Automatic Differentiation [4], [9], [10]	Auto-diff	Medium	Slow/Medium	High
<i>Analytical Lagrangian Differentiation</i> [13], [14]	Lag-diff	Hard	Medium/Fast	High
Analytical Chain-Rule Differentiation [6], [15]	Chain-rule diff	Hard	Medium	High

TABLE I: Summary of methods to calculate partial derivatives of rigid-body dynamics. This paper belongs to the category *Analytical Lagrangian Differentiation*, and is *Fast* in the speed category.

expressions for the first-order partial derivative of the inverse dynamics with an algorithm of order $\mathcal{O}(Nd)$, and then use the relationship between forward and inverse dynamics [6], [14] in an efficient manner to ultimately calculate the partial derivatives of forward dynamics. The order of this new method is $\mathcal{O}(N^2)$. Benefits of our method over that from Ref. [14] include the extension to branched trees, several improved algorithmic efficiencies, and a direct pathway to the second-order partial derivatives, an innovation of particular interest to the authors. We further supply a generalization of this algorithm to the case of multi-DoF joints, as is needed to treat floating-base systems. For all the theoretical development, Featherstone’s Spatial Vector Algebra [16] is used.

II. PARTIAL DERIVATIVES OF RIGID-BODY DYNAMICS

For a rigid-body system, the state variables are the generalized position vector \mathbf{q} and the generalized velocity vector $\dot{\mathbf{q}}$, while the control variable is the generalized torque vector $\boldsymbol{\tau}$. The equation of motion of such a system, also called its Inverse Dynamics (*ID*), is given by

$$\boldsymbol{\tau} = \mathbf{M}(\mathbf{q})\ddot{\mathbf{q}} + \mathbf{C}(\mathbf{q}, \dot{\mathbf{q}})\dot{\mathbf{q}} + \mathbf{g}(\mathbf{q}) \quad (1)$$

$$= ID(model, \mathbf{q}, \dot{\mathbf{q}}, \ddot{\mathbf{q}}) \quad (2)$$

where \mathbf{M} is the mass matrix, \mathbf{C} is a Coriolis matrix, and \mathbf{g} is the vector of generalized gravitational forces. For a fixed state, the Inverse Dynamics (*ID*) calculate $\boldsymbol{\tau}$ for a given $\ddot{\mathbf{q}}$ (Eq. 1), and Forward Dynamics (*FD*) compute $\ddot{\mathbf{q}}$ for a given $\boldsymbol{\tau}$ via

$$\ddot{\mathbf{q}} = \mathbf{M}^{-1}(\mathbf{q}) (\boldsymbol{\tau} - \mathbf{C}(\mathbf{q}, \dot{\mathbf{q}})\dot{\mathbf{q}} - \mathbf{g}(\mathbf{q})) \quad (3)$$

$$= FD(model, \mathbf{q}, \dot{\mathbf{q}}, \boldsymbol{\tau}) \quad (4)$$

Toward supporting control applications (e.g., [1], [8]), the objective of this work is to compute the partial derivatives of the *FD* with respect to the state $(\mathbf{q}, \dot{\mathbf{q}})$ and control variables $(\boldsymbol{\tau})$. The most efficient algorithms for calculating *ID* and *FD* are the Recursive Newton-Euler Algorithm (RNEA) and the Articulated-Body Algorithm (ABA) respectively [16]. Both of these algorithms are of order $\mathcal{O}(N)$.

A. Analytical Derivative of Dynamics

The state-of-the-art analytical method [6] for computing partial derivatives of *FD* uses chain rule differentiation of the RNEA algorithm (FDCR, Table II), and then use a relation between *FD* and *ID* [6], [14] as:

$$\left. \frac{\partial FD}{\partial u} \right|_{\mathbf{q}_0, \dot{\mathbf{q}}_0, \boldsymbol{\tau}_0} = -\mathbf{M}^{-1}(\mathbf{q}_0) \left. \frac{\partial ID}{\partial u} \right|_{\mathbf{q}_0, \dot{\mathbf{q}}_0, \ddot{\mathbf{q}}_0} \quad (5)$$

The variable $u \in \{\mathbf{q}, \dot{\mathbf{q}}\}$, and the partials of *FD* and *ID* can be calculated for any particular value of the state variables. In this paper, Eq. 5 is referred to as the inverse partial relation (IPR).

A direct approach to compute the partial derivatives of *FD* is to directly manually differentiate the ABA algorithm via the chain-rule, called ABACR (Table II). However, because the ABA has three main loops, compared to the two loops of RNEA, the more efficient FDCR (Table II) first differentiates RNEA via chain-rule and then uses Eq. 5 to back out the partials of *FD* [6].

In this paper, a new and even more efficient method (FDSVA, Table II) for branched kinematic trees is presented for calculating these *FD* partials. The new method utilizes the *ID* efficiencies similar to Ref. [6], [14], but additionally exploits kinematic identities, spatial vector algebra, and a variety of implementation optimizations to reduce computational burden.

III. SPATIAL VECTOR ALGEBRA (SVA) AND PROPERTIES

A spatial vector is defined as a 6D vector that combines the linear and angular aspects of a rigid-body motion or net force [16]. In this paper, spatial vectors are denoted with lower-case bold letters (for example, \mathbf{a}), while matrices are denoted as capitalized bold letters (for example, \mathbf{A}). Motion vectors, such as velocity and acceleration, belong to a 6D vector space denoted M^6 . Force-like vectors, like force and momentum, belong to another 6D vector space F^6 , which is the dual of M^6 . A cross-product between two motion vectors is written as $\mathbf{m}_1 \times \mathbf{m}_2$, and a cross-product between a motion and a force vector is written as $\mathbf{m} \times^* \mathbf{f}$. An operator $\bar{\times}^*$ is obtained by swapping the order of the cross product, and is defined as $(\mathbf{f} \bar{\times}^*) \mathbf{v} = (\mathbf{v} \bar{\times}^*) \mathbf{f}$ [18]. Hence, all the vector cross-product operators used are: [16]

$$\begin{aligned}
\times &: M^6 \times M^6 \rightarrow M^6 \\
\times^* &: M^6 \times F^6 \rightarrow F^6 \\
\bar{\times}^* &: F^6 \times M^6 \rightarrow F^6
\end{aligned} \tag{6}$$

A fixed-base open-chain kinematic tree with serial or branched connectivity (Fig. 1) is considered with N links connected by single-DoF joints (e.g., such as revolutes). Body i 's parent body is denoted as $\lambda(i)$ and is towards the root of the kinematic tree. We define $i \leq j$ if body i is in the path from body j towards the base. The vector \mathbf{v}_k is the spatial velocity vector for body k , and ϕ_k is the joint motion axis vector for body k , used to calculate the joint velocity as $\mathbf{v}_{J_k} = \phi_k \dot{q}_k$. The matrix \mathbf{I}_k denotes the spatial inertia for body k [16].

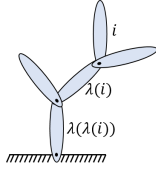


Fig. 1: N -link open-chain kinematic tree with parent-child link notation.

Several kinematic identities are derived for open-chain kinematic trees with branched or serial connectivity when spatial vectors are expressed in the ground frame. The derivative of joint motion vector due to the axis changing with respect to local coordinates (commonly denoted $\dot{\phi}_i$ [16]) is assumed to be zero. Several properties from Ref. [16] are used. Identity I1 below is used to derive the rest of the identities presented. I2 gives the rate of change of joint motion vector (ϕ_k) for body k , with respect to the change in the joint angle (q_j) of joint j . The value is non-zero only if body j lies in the path of body k and the base. Identity I3 on the other hand gives the rate of change of spatial velocity of body k by perturbing joint angle for body j . These identities are used extensively throughout and are listed as follows.

$$\begin{aligned}
\text{I1. } \frac{\partial \mathbf{X}_i}{\partial q_j} &= \begin{cases} \phi_j \times \mathbf{X}_i, & \text{if } j \leq i \\ 0, & \text{otherwise} \end{cases} \\
\text{I2. } \frac{\partial \phi_k}{\partial q_j} &= \begin{cases} \phi_j \times \phi_k, & \text{if } j \leq k \\ 0, & \text{otherwise} \end{cases} \\
\text{I3. } \frac{\partial \mathbf{v}_k}{\partial q_j} &= \begin{cases} \phi_j \times (\mathbf{v}_k - \mathbf{v}_j), & \text{if } j \leq k \\ 0, & \text{otherwise} \end{cases} \\
\text{I4. } \frac{\partial \mathbf{v}_k}{\partial \dot{q}_j} &= \begin{cases} \phi_j, & \text{if } j \leq k \\ 0, & \text{otherwise} \end{cases} \\
\text{I5. } \frac{\partial \mathbf{I}_k}{\partial q_j} &= \begin{cases} \phi_j \times^* \mathbf{I}_k - \mathbf{I}_k (\phi_j \times), & \text{if } j \leq k \\ 0, & \text{otherwise} \end{cases} \\
\text{I6. } \frac{\partial \xi_k}{\partial q_j} &= \begin{cases} (\phi_j \times) (\xi_k - \xi_j) \\ \quad + \phi_j \times (\mathbf{v}_k - \mathbf{v}_j), & \text{if } j \leq k \\ 0, & \text{otherwise} \end{cases}
\end{aligned}$$

$$\begin{aligned}
\text{I7. } \frac{\partial \xi_k}{\partial \dot{q}_j} &= \begin{cases} \dot{\phi}_j + \phi_j \times (\mathbf{v}_k - \mathbf{v}_j), & \text{if } j \leq k \\ 0, & \text{otherwise} \end{cases} \\
\text{I8. } \frac{\partial \gamma_k}{\partial q_j} &= \begin{cases} \phi_j \times (\gamma_k - \gamma_j), & \text{if } j \leq k \\ 0, & \text{otherwise} \end{cases}
\end{aligned}$$

The matrix \mathbf{X}_i is the coordinate transformation matrix for transforming motion vectors from body i 's coordinates to base coordinates (also written as ${}^0\mathbf{X}_i$). Vectors $\mathbf{v}_k = \sum_{l \leq k} \phi_l \dot{q}_l$, and $\dot{\phi}_k = \mathbf{v}_k \times \phi_k$, where \mathbf{v}_k denotes the spatial velocity of body k . The quantities $\xi_k = \sum_{l \leq k} \mathbf{v}_l \times \phi_l \dot{q}_l$ and $\gamma_k = \sum_{l \leq k} \phi_l \dot{q}_l$ decompose the body acceleration \mathbf{a}_k into terms from joint accelerations, and terms from joint rates, such that $\mathbf{a}_k = \gamma_k + \xi_k$.

IV. ANALYTICAL PARTIAL DERIVATIVES USING SVA

The first-order partial derivative of FD with respect to the control variable τ is straightforward from Eq. 3.

$$\frac{\partial \ddot{\mathbf{q}}}{\partial \tau} = \mathbf{M}^{-1}(\mathbf{q}) \tag{7}$$

A. First-order Partial Derivatives of ID w.r.t. \mathbf{q}

Taking the first-order partial derivative of ID (Eq. 1) with respect to \mathbf{q} gives:

$$\frac{\partial \tau}{\partial \mathbf{q}} = \frac{\partial [\mathbf{M}(\mathbf{q})]}{\partial \mathbf{q}} \ddot{\mathbf{q}} + \frac{\partial [\mathbf{C}(\mathbf{q}, \dot{\mathbf{q}})]}{\partial \mathbf{q}} \dot{\mathbf{q}} + \frac{\partial g(\mathbf{q})}{\partial \mathbf{q}} \tag{8}$$

Computing $\frac{\partial [\mathbf{M}(\mathbf{q})]}{\partial \mathbf{q}}$ and $\frac{\partial [\mathbf{C}(\mathbf{q}, \dot{\mathbf{q}})]}{\partial \mathbf{q}}$ in Eq. 8 can be accomplished via a $\mathcal{O}(Nd^2)$ algorithm. Instead of this expensive formulation that requires tensor algebra, we instead combine the matrix vector product before taking the partial of Eq. 1. Noting that $\ddot{\mathbf{q}}$, and $\dot{\mathbf{q}}$ are independent of \mathbf{q} :

$$\frac{\partial \tau}{\partial \mathbf{q}} = \frac{\partial [\mathbf{M}(\mathbf{q}) \ddot{\mathbf{q}}]}{\partial \mathbf{q}} + \frac{\partial [\mathbf{C}(\mathbf{q}, \dot{\mathbf{q}}) \dot{\mathbf{q}}]}{\partial \mathbf{q}} + \frac{\partial g(\mathbf{q})}{\partial \mathbf{q}} \tag{9}$$

The generalized force for joint i is given as

$$\tau_i = \phi_i^T \mathbf{f}_i^B \tag{10}$$

where \mathbf{f}_i^B is the spatial force transmitted from parent body to body i across joint i . From the formulation of the the RNEA [16] we know that,

$$\tau_i = \phi_i^T \sum_{k \geq i} \mathbf{I}_k \mathbf{a}_k + \mathbf{v}_k \times^* \mathbf{I}_k \mathbf{v}_k \tag{11}$$

where, \mathbf{v}_k is the spatial velocity of body k ,

$$\mathbf{v}_k = \sum_{l \leq k} \phi_l \dot{q}_l \tag{12}$$

and \mathbf{a}_k is the spatial acceleration of the body k :

$$\mathbf{a}_k = \sum_{l \leq k} \phi_l \ddot{q}_l + \mathbf{v}_l \times \phi_l \dot{q}_l \tag{13}$$

In the expanded Lagrangian form, Eq. 1 is written as:

$$\tau_i = \sum_{j=1}^N M_{ij}(q)\ddot{q}_j + \sum_{j=1}^N C_{ij}(q)\dot{q}_j + g_i(q) \quad (14)$$

For any particular joint i in the rigid-body system, Eq. 14 can be written as follows.

$$\tau_i = [\mathbf{M}(q)\ddot{\mathbf{q}}]_i + [\mathbf{C}(q, \dot{\mathbf{q}})\dot{\mathbf{q}}]_i + g_i(q) \quad (15)$$

Then, using Eq. 11, 12, 13, and 15, the expressions for the scalar terms $[\mathbf{M}(q)\ddot{\mathbf{q}}]_i$ and $[\mathbf{C}(q, \dot{\mathbf{q}})\dot{\mathbf{q}}]_i$ reduce to:

$$[\mathbf{M}(q)\ddot{\mathbf{q}}]_i = \phi_i^T \sum_{k \geq i} [\mathbf{I}_k \gamma_k] \quad (16)$$

$$[\mathbf{C}(q, \dot{\mathbf{q}})\dot{\mathbf{q}}]_i = \phi_i^T \sum_{k \geq i} [\mathbf{v}_k \times^* \mathbf{I}_k \mathbf{v}_k + \mathbf{I}_k \boldsymbol{\xi}_k] \quad (17)$$

The subsequent derivations employ these formulae along with the previous identities to obtain the partials of each term in Eq. 15.

Partial Derivative of Eq. 16: To get the partial derivative of $[\mathbf{M}(q)\ddot{\mathbf{q}}]_i$ with respect to q_j for all $i, j \in \{1, \dots, N\}$, suppose $j \leq i$. Using the identities I2, I5, and I8 (see Section III) leads to:

$$\frac{\partial [\mathbf{M}(q)\ddot{\mathbf{q}}]_i}{\partial q_j} = \phi_i^T [\mathbf{I}_i^C (\gamma_j \times \phi_j)] \quad (18)$$

For the case $i \leq j$, we use the identities I5, I8 to get:

$$\frac{\partial [\mathbf{M}(q)\ddot{\mathbf{q}}]_i}{\partial q_j} = \phi_i^T [(\phi_j \times^*) \boldsymbol{\eta}_j^C + \mathbf{I}_j^C (\gamma_j \times \phi_j)] \quad (19)$$

where $\boldsymbol{\eta}_l = \mathbf{I}_l \gamma_l$ is defined as the spatial force on the body caused by acceleration due to joint accelerations $\ddot{\mathbf{q}}$. The matrix \mathbf{I}_j^C denotes the composite rigid-body inertia of the sub-tree rooted at body j , given by $\mathbf{I}_j^C = \sum_{l \geq j} \mathbf{I}_l$. Similarly, $\boldsymbol{\eta}_j^C$ collects joint-acceleration-dependent forces for the subtree, calculated as $\boldsymbol{\eta}_j^C = \sum_{l \geq j} \boldsymbol{\eta}_l$.

For ease of implementation, we consider a single case where $j \leq i$. The indices i and j are switched in Eq. 19, to get the expression for $\frac{\partial [\mathbf{M}(q)\ddot{\mathbf{q}}]_j}{\partial q_i}$ for the case $j \leq i$. Therefore, Eq. 20 gives the two expressions formulated for the general case $j \leq i$.

$$\begin{aligned} \frac{\partial [\mathbf{M}(q)\ddot{\mathbf{q}}]_i}{\partial q_j} &= -\phi_j^T [\gamma_j \times^* \mathbf{I}_i^C \phi_i] \\ \frac{\partial [\mathbf{M}(q)\ddot{\mathbf{q}}]_j}{\partial q_i} &= \phi_j^T [(\phi_i \times^*) \boldsymbol{\eta}_i^C + \mathbf{I}_i^C (\gamma_i \times \phi_i)] \end{aligned} \quad (20)$$

Partial Derivative of Eq. 17: Similarly, we use identities I3, I5 and I6 (Section III) to get the first-order partial derivative of $[\mathbf{C}(q, \dot{\mathbf{q}})\dot{\mathbf{q}}]_i$ with respect to q_j for the case $i \leq j$ as:

$$\begin{aligned} \frac{\partial [\mathbf{C}\dot{\mathbf{q}}]_i}{\partial q_j} &= \phi_i^T [2\mathbf{B}_j^C \dot{\phi}_j - \mathbf{I}_j^C (\phi_j \times) \boldsymbol{\xi}_j \\ &\quad + \mathbf{I}_j^C (\mathbf{v}_j \times) \dot{\phi}_j + (\phi_j \times^*) \boldsymbol{\zeta}_j^C] \end{aligned} \quad (21)$$

The variable $\boldsymbol{\zeta}_l$ is defined as $\boldsymbol{\zeta}_l = \mathbf{v}_l \times^* \mathbf{I}_l \mathbf{v}_l + \mathbf{I}_l \boldsymbol{\xi}_l$, and gives the Coriolis and centripetal forces on body l . Its composite for the subtree is defined as $\boldsymbol{\zeta}_j^C = \sum_{l \geq j} \boldsymbol{\zeta}_l$. Finally, the matrix $\mathbf{B}_l(\mathbf{v}_l, \mathbf{I}_l)$ is given by:

$$\mathbf{B}_l = \frac{1}{2} [(\mathbf{v}_l \times^*) \mathbf{I}_l - \mathbf{I}_l (\mathbf{v}_l \times) + (\mathbf{I}_l \mathbf{v}_l) \bar{\times}^*] \quad (22)$$

with its composite $\mathbf{B}_j^C = \sum_{l \geq j} \mathbf{B}_l$. This definition of $\mathbf{B}_l(\mathbf{v}_l, \mathbf{I}_l)$ was proposed by Niemeyer and Slotine [19], [20] as a way to factorize the bi-linear term in the spatial equation of motion. This term is expected in the first order partial derivative of $[\mathbf{C}(q, \dot{\mathbf{q}})\dot{\mathbf{q}}]_i$, since one definition of \mathbf{C}_{ij} by Ref. [18], for the case $i \leq j$, is:

$$\begin{aligned} \mathbf{C}_{ij} &= \phi_i^T (\mathbf{I}_j^C \dot{\phi}_j + \mathbf{B}_j^C \phi_j) \\ \mathbf{C}_{ji} &= \phi_j^T \mathbf{I}_j^C \dot{\phi}_i + \phi_j^T \mathbf{B}_j^C \phi_i \end{aligned} \quad (23)$$

Again, using the identities I3, I5 and I6 (Section III), the partial derivative of $[\mathbf{C}(q, \dot{\mathbf{q}})\dot{\mathbf{q}}]_i$ with respect to q_j for the case $j \leq i$ is:

$$\frac{\partial [\mathbf{C}\dot{\mathbf{q}}]_i}{\partial q_j} = \phi_i^T [2\mathbf{B}_i^C \dot{\phi}_j - \mathbf{I}_i^C (\phi_j \times) \boldsymbol{\xi}_j + \mathbf{I}_i^C (\mathbf{v}_j \times) \dot{\phi}_j] \quad (24)$$

Similar to previously, i and j are switched in Eq. 21 to get the expression for $\frac{\partial [\mathbf{C}\dot{\mathbf{q}}]_j}{\partial q_i}$ for the case $j \leq i$ giving:

$$\begin{aligned} \frac{\partial [\mathbf{C}\dot{\mathbf{q}}]_i}{\partial q_j} &= 2\phi_i^T \mathbf{B}_i^C \dot{\phi}_j + \phi_i^T \mathbf{I}_i^C [\boldsymbol{\xi}_j \times \phi_j + \mathbf{v}_j \times \dot{\phi}_j] \\ \frac{\partial [\mathbf{C}\dot{\mathbf{q}}]_j}{\partial q_i} &= \phi_j^T [2\mathbf{B}_i^C \dot{\phi}_i + \mathbf{I}_i^C (\boldsymbol{\xi}_i \times \phi_i + \mathbf{v}_i \times \dot{\phi}_i) \\ &\quad + \phi_i \times^* \boldsymbol{\zeta}_i^C] \end{aligned} \quad (25)$$

Partial Derivative of the Gravity Term: Instead of treating the gravity as an external force, the base is assumed to be accelerated upwards with the gravitational acceleration ($\mathbf{a}_0 = -\mathbf{a}_g$). The generalized force due to gravity [16], g_i at any body i in a kinematic chain is:

$$g_i = \phi_i^T \mathbf{I}_i^C \mathbf{a}_{g_i} \quad (26)$$

where \mathbf{a}_{g_i} is the spatial acceleration opposite gravity on body i (i.e., $\mathbf{a}_{g_i} = -\mathbf{a}_g$). For the case $j \leq i$, the partial derivative of g_i with respect to q_j is:

$$\frac{\partial g_i}{\partial q_j} = -\phi_i^T (\mathbf{I}_i^C (\phi_j \times)) \mathbf{a}_{g_i} \quad (27)$$

For the case $i \leq j$, the partial is:

$$\frac{\partial g_i}{\partial q_j} = \phi_i^T (\phi_j \times^* \mathbf{I}_j^C - \mathbf{I}_j^C (\phi_j \times)) \mathbf{a}_{g_i} \quad (28)$$

Again, the indices i and j are switched for the case in Eq. 28. Eq. 29 gives $\frac{\partial g_j}{\partial q_i}$ for the case $j \leq i$.

$$\frac{\partial g_j}{\partial q_i} = \phi_j^T (\phi_i \times^* \mathbf{I}_i^C - \mathbf{I}_i^C (\phi_i \times)) \mathbf{a}_{g_i} \quad (29)$$

Since g_i is a conservative force, the following symmetry condition holds for the Jacobian matrix $\frac{\partial g_i}{\partial q_j}$.

$$\frac{\partial g_i}{\partial q_j} = \frac{\partial g_j}{\partial q_i} \quad (30)$$

Due to the condition in Eq. 30, either Eq. 27 or Eq. 29 is used to calculate $\frac{\partial g_i}{\partial q_j}$. Equation 27 is re-arranged as follows to better suit the algorithm:

$$\frac{\partial g_i}{\partial q_j} = -\phi_j^T (\mathbf{a}_{g_i} \times^* \mathbf{I}_i^C \phi_i) \quad (31)$$

Summary for Partial of ID w.r.t. q : The partials of the individual components are now collected together. We consider the acceleration \mathbf{a}_k is of body k , redefined to include the gravity bias as:

$$\mathbf{a}_k = \gamma_k + \xi_k + \mathbf{a}_{g_k} \quad (32)$$

The net spatial force on body k is then defined as:

$$\mathbf{f}_k = \boldsymbol{\eta}_k + \zeta_k + \mathbf{I}_k \mathbf{a}_{g_k} \quad (33)$$

Using Eq 32, and the definitions of $\boldsymbol{\eta}_k$ and ζ_k recovers:

$$\mathbf{f}_k = \mathbf{I}_k \mathbf{a}_k + \mathbf{v}_k \times^* \mathbf{I}_k \mathbf{v}_k \quad (34)$$

Using Eq. 9, terms in Eqs. 20, 25, 29, and 31 are added to get the total expressions for $\frac{\partial \tau}{\partial q}$ for the case $j \leq i$.

$$\begin{aligned} \frac{\partial \tau_i}{\partial q_j} &= \dot{\phi}_j^T [2\mathbf{B}_i^C]^\top \phi_i + \ddot{\phi}_j^T \mathbf{I}_i^C \phi_i \\ \frac{\partial \tau_j}{\partial q_i} &= \phi_j^T [2\mathbf{B}_i^C \dot{\phi}_i + \mathbf{I}_i^C \ddot{\phi}_i + (\phi_i \times^* \mathbf{f}_i^C)] \end{aligned} \quad (35)$$

where \mathbf{f}_i^C is the composite force \mathbf{f} on the sub-tree at body i , defined as $\mathbf{f}_i^C = \sum_{l \geq i} \mathbf{f}_l$. The vector $\dot{\phi}_i$ is defined as $\dot{\phi}_i = \mathbf{a}_i \times \phi_i + \mathbf{v}_i \times \dot{\phi}_i$, and physically is the rate of change of ϕ_i in the global coordinate frame.

B. First-Order Partial Derivatives of ID w.r.t. \dot{q}

The partials of τ with respect to \dot{q} are closely related to a special factorization of the Coriolis terms $\mathbf{C}\dot{q}$. Using Ref. [18, Remark 2], for the proper choice of \mathbf{C} , then $\mathbf{C} = \frac{1}{2} \frac{\partial \tau}{\partial \dot{q}}$. Using this result, identities I4, I7, and Eq. 23 leads to expressions for the case when $j \leq i$ is:

$$\begin{aligned} \frac{\partial \tau_i}{\partial \dot{q}_j} &= \frac{\partial [\mathbf{C}\dot{q}]_i}{\partial \dot{q}_j} = 2\phi_i^T \mathbf{B}_i^C \phi_j + 2\dot{\phi}_j^T \mathbf{I}_i^C \phi_i \\ \frac{\partial \tau_j}{\partial \dot{q}_i} &= \frac{\partial [\mathbf{C}\dot{q}]_j}{\partial \dot{q}_i} = 2\phi_j^T [\mathbf{B}_i^C \phi_i + \mathbf{I}_i^C \dot{\phi}_i] \end{aligned} \quad (36)$$

C. Algorithm for First-Order Partial of ID

Algorithm 1, detailed in the Appendix, returns the terms in Eq. 35 and Eq. 36 and has computational complexity $\mathcal{O}(Nd)$. The first pass is in the forward direction and goes from root to leaves calculating the spatial velocity, acceleration and the force, equivalent to RNEA. The second pass progresses in the backward direction from leaves to the root. Index i takes all the values from 1 to N , and index j goes through $i, \lambda(i)$, and so on, back to the root of the tree. Inside the second pass, the composite quantities \mathbf{I}^C , \mathbf{B}^C , and \mathbf{f}^C are calculated recursively for each sub-tree. Common terms like \mathbf{B}_i^C and $(\mathbf{I}_i^C \phi_i)$ in Eq. 35 and Eq. 36 are evaluated only once and re-used to build an efficient algorithm. The final form of the algorithm is found to bear a great deal of resemblance to Algorithm 2 in [14], however, the derivation here is tailored for branched trees, further optimized as considered in the next section, and compared with chain-rule approaches for the first time.

V. IMPLEMENTATION CONSIDERATIONS

A. Relating Partial of FD and ID

Equation 5 (IPR) gives the relation between the derivative of FD and ID , where $\frac{\partial ID}{\partial \mathbf{u}}$ ($\mathbf{u} = [q, \dot{q}]$) is an $N \times 2N$ matrix, and \mathbf{M}^{-1} is an $N \times N$ matrix. A direct multiplication of the two matrices results into an $\mathcal{O}(N^3)$ operation. A less expensive $\mathcal{O}(N^2)$ method to calculate the product of \mathbf{M}^{-1} with $\frac{\partial ID}{\partial \mathbf{u}}$ is presented in this section.

ABA gives \ddot{q} (Eq. 3) for a given τ , represented as:

$$\ddot{q} = ABA(q, \dot{q}, \tau, \mathbf{a}_g) \quad (37)$$

From Eq. 3, for $\dot{q} = \mathbf{0}$, $g = \mathbf{0}$ and an arbitrary input vector $\tau = \mathbf{b}$, \ddot{q} results in:

$$\ddot{q} = \mathbf{M}^{-1} \mathbf{b} \quad (38)$$

The product of the matrix \mathbf{M}^{-1} with any column vector \mathbf{b} can therefore be calculated by using ABA with $\dot{q} = \mathbf{0}$, $g = \mathbf{0}$, and input vector \mathbf{b} :

$$\mathbf{M}^{-1} \mathbf{b} = ABA(q, \mathbf{0}, \mathbf{b}, \mathbf{0}) \quad (39)$$

For a product of \mathbf{M}^{-1} with any given matrix (of size $N \times m$), ABA can be used m times with $\dot{q} = \mathbf{0}$, $g = \mathbf{0}$ and \mathbf{b} as the column vectors of the given matrix one at a time, resulting in an $\mathcal{O}(Nm)$ operation. Due to the repeated use of ABA for each input column vector, the kinematic variables and bias force are only calculated once in the first forward loop, and saved for re-use. To implement Eq. 5, Eq. 39 is used with \mathbf{b} as the column vectors of $\frac{\partial ID}{\partial \mathbf{u}}$ one at a time. This process is defined as the "ABA-Zero-Algorithm" (AZA), since inputs \dot{q} and g are $\mathbf{0}$. Fig. 2 compares DMM (Table II) with AZA for open-loop serial kinematic chains. The DMM subroutine uses

the open-source BLAS [21] matrix multiplication library Level-3 subroutine `DSYMM`. In Fig. 2, the "crossover" N denotes the point below which the DMM performs better than the AZA. This point depends on the hardware and compiler optimization settings used to implement the algorithm, but for very high N , the $\mathcal{O}(N^2)$ AZA is efficient because it avoids the expensive matrix-matrix product. For M^{-1} required in Eq. 7, we loop over the AZA with input vectors as columns of an identity matrix.

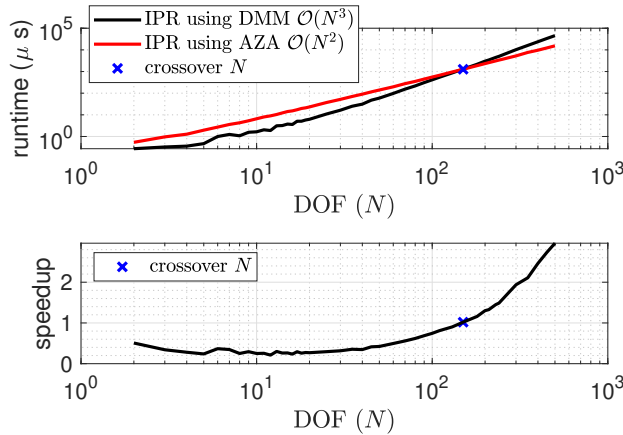


Fig. 2: a) Direct Matrix Multiplication ($\mathcal{O}(N^3)$) outperforms AZA ($\mathcal{O}(N^2)$) below the crossover " N " for IPR Eq. 5. b) Speedup plot shows the speedup of AZA to DMM

B. Body Frame vs Ground Frame Algorithms

Since SVA allows for coordinate-free expressions, recursive algorithms can be formulated in either body-coordinates or ground-coordinates [16]. For the body-coordinate algorithms, all the intermediate quantities are transformed between body coordinates using transformation matrices ${}^i X_{\lambda(i)}$, while for the ground-coordinates algorithms, the quantities can be left in the ground frame. A big advantage for the latter comes by avoiding the repeated transformation of the quantities between local body frames in the nested loops of the recursive algorithm. This gain is achieved at the cost of expressing kinematic quantities (velocity ${}^0 v_i$, acceleration ${}^0 a_i$), joint

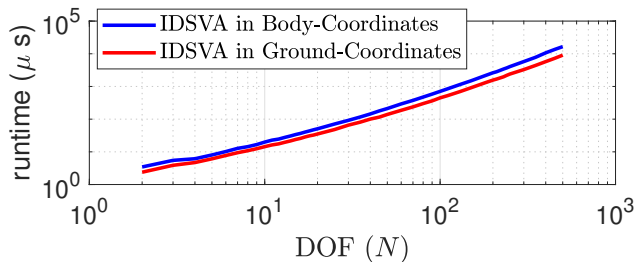


Fig. 3: IDSVA (Table II) in Body-coordinates vs. in Ground-coordinates

motion vector ${}^0 \phi_i$ and inertia matrices ${}^0 I_i$ in the ground coordinate frame during the first outward pass. Fig. 3 shows a comparison of IDSVA (see Table II) runtime in body coordinates and ground coordinates. Speedups for ground coordinate algorithms are between 1.3 to 1.9 for $N = 2$ to $N = 500$. The ground coordinates algorithm is moderately faster due to the nested loop in the second pass of the algorithm.

VI. COMPARISON RESULTS

A. CPU Runtimes for Partial of ID

We consider an N link serial kinematic tree with all revolute joints about their local z -axis. For each link, the mass is 1 kg, the length is 1 m and the center of mass is located at the midpoint. The inertia about the z -axis is $I_{zz} = 1 \text{ kg m}^2$, while inertia about other axes, and cross-inertia values are 0 kg m^2 . RNEACR in body-coordinates [6] (Table II) is used to calculate the partial derivatives of ID , and compared with the new IDSVA (Table II) method. All algorithms are written in Fortran 90 and implemented using the Intel Fortran compiler on a 3.07 Ghz Intel Xeon processor. To calculate the average run time, each algorithm is run 10,000 times with randomized inputs for the state and control variables. Fig. 4 shows the comparison of the two methods. For $N = 100$, a speedup of $15\times$ is found.

Preliminary results with a generalization of our algorithm to multi degree of freedom joints is shown in Fig. 5 using the Pinocchio [22] C++ framework with the GCC compiler. For a 36 link floating-base humanoid, IDSVA has a speedup of 1.6x over RNEACR [6]. The smaller speedup compared to the Fortran results is a testament to the extreme efficiency of the RNEACR implementation of [6] in Pinocchio. For example, the use of world coordinates in the implementation of [6] appears to offer more significant savings than with IDSVA. It is worth noting that the implementation of our own IDSVA algorithm in Pinocchio has benefited a great deal from the overall architecture of the Pinocchio code (in terms of its efficient implementation of spatial vector operations and other benefits derived from its use of the curiously recurring template pattern (CRTP) throughout). However, the comparison with both implementations considered on top of a common code base also helps to confirm that the IDSVA algorithm itself is more efficient than RNEACR. More detailed comparison for multi-dof joint models along with theoretical development will be presented in future publications. An open source Pinocchio implementation of IDSVA for multi-dof joint models is available here:

<https://github.com/pwensing/pinocchio>

and an open source MATLAB implementation is here:

https://github.com/ROAM-Lab-ND/spatial_v2_extended

Algorithm/Methods	Description	Abbreviation
Algorithms		
RNEA first order chain-rule	chain-rule of RNEA to calculate partial derivative of ID	RNEACR
ID first order partial using SVA	partial derivative of ID using SVA method described in this paper (Algo 1)	IDSVA
FD first order partial using ABA chain-rule	chain-rule of ABA to calculate partial derivative of FD	ABACR
FD first order partial using RNEA chain-rule and IPR (using DMM)	method for calculating first order partial derivative of FD using RNEACR, IPR (using DMM), and M^{-1} [6]	FDCR
FD first order partial using SVA and IPR	method for calculating first order partial derivative of FD using IDSVA, IPR (using DMM/AZA), and M^{-1}	FDSVA
Supporting Methods		
$\frac{\partial FD}{\partial u} = -M^{-1} \frac{\partial ID}{\partial u}$	relation between partial derivative of FD and ID	IPR
ABA-Zero-Algorithm	ABA with $\dot{q} = \mathbf{0}$, $g = \mathbf{0}$	AZA
Direct Matrix Multiplication	$\mathcal{O}(N^3)$ operation for matrix multiplication (order N) using BLAS	DMM

TABLE II: Abbreviations of various algorithms/methods used. The bold acronyms are presented in the current paper.

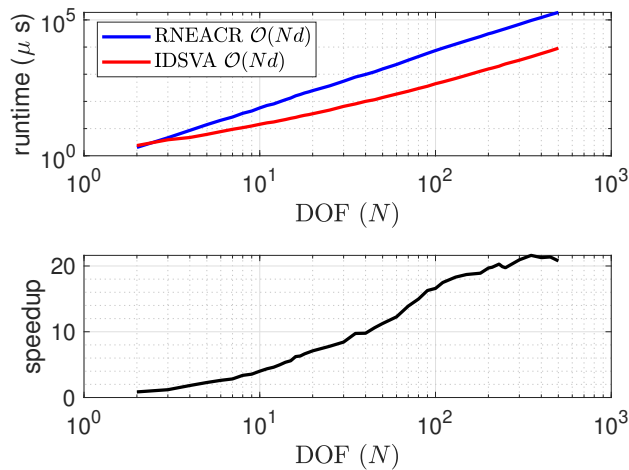


Fig. 4: IDSVA outperforms RNEACR (Table II) for all $N \geq 2$

B. CPU Runtimes For Partial Derivatives of FD

Figure 6 shows the distribution of subcomponent timings for the FDSVA (Table II) method. The point of intersection of the curves IDSVA (green) and IPR using DMM (black) is called the “order switch” N . Below this N , the $\mathcal{O}(Nd)$ IDSVA algorithm dominates the runtime. Above the “order switch” N , the $\mathcal{O}(N^3)$ application of the IPR using DMM (black) dominates the runtime, but is still faster (for all points below crossover N) than the $\mathcal{O}(N^2)$ application of the IPR using the AZA (red). The method switches to using the AZA in place of DMM for the IPR at the “crossover N ”, and the application of the IPR continues to dominate the runtime. Due to these two points, a slight inflection point is visible in the runtime of FDSVA in Fig. 6. The magenta curve shows the $\mathcal{O}(N^2)$ calculation of M^{-1} (required in Eq. 7) based on the AZA. Overall, the FDSVA method has the

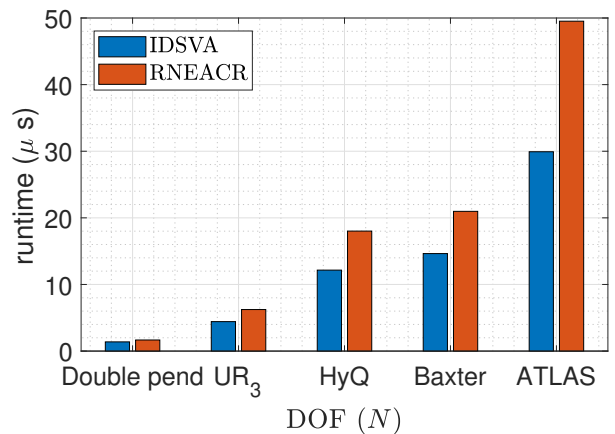


Fig. 5: Comparison of IDSVA with RNEACR in Pinocchio [22] framework for several floating base multi-dof robots a) Fixed base double pendulum ($N=2$), b) Fixed base UR₃ ($N=6$), c) Floating base HyQ ($N=19$), d) Fixed base Baxter ($N=19$), e) Floating base ATLAS ($N=36$)

computational complexity of $\mathcal{O}(N^2)$.

Fig. 7 shows a summary of comparison in the CPU runtimes for the three methods (ABACR, FDCR, FDSVA (Table II)) of calculating the partial derivatives of FD . With the analytical derivative expressions developed herein, FDSVA method outperforms both the compared methods for all values of $N \geq 2$. For theoretical purposes, the runtimes were tested for cases up to $N=1,000$. The desktop machine ran out for memory for cases more than $N=500$, but tests on a different machine with more memory showed similar trends as shown in Fig 7 after the “crossover” N .

The partial derivatives from the three methods were compared with derivatives calculated using the complex-step method for accuracy. For the $N=100$ link case, the ABACR method results in a term-by-term root-mean-

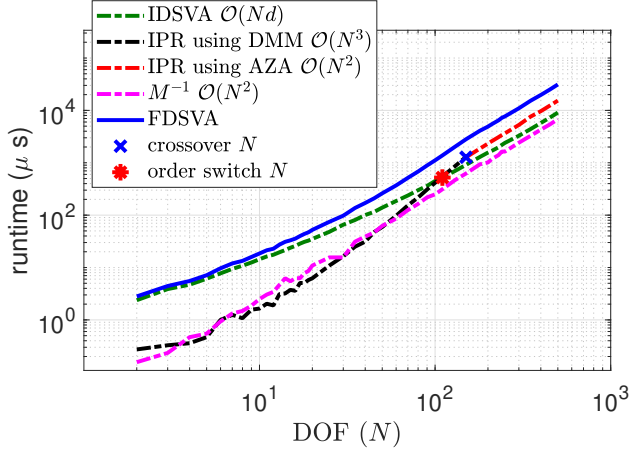


Fig. 6: CPU runtime composition for FDSVA method. Runtime for FDSVA = runtime (IDSVA) + runtime (IPR)+ runtime (M^{-1})

square (rms) relative error of 10^{-13} , while both FDSVA and FDCR result in an rms error of approximately 10^{-12} . Further accuracy analyses of the partial derivatives will be provided in future work.

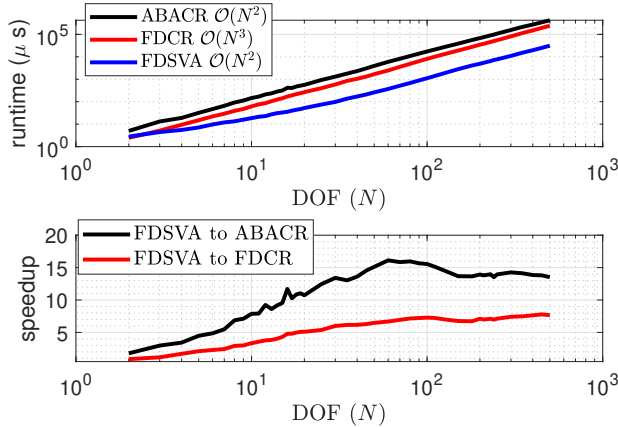


Fig. 7: a) CPU runtime comparison of methods for the first-order partial derivatives of FD . b) Speedup plots show FDSVA outperforms both ABACR and FDCR

VII. CONCLUSIONS

In this work, we present an efficient algorithm using Spatial Vector Algebra (SVA) to calculate accurate partial derivatives of forward and inverse dynamics for branched kinematic trees. Several algorithmic optimizations and SVA identities are exploited to enable an efficient implementation. The Fortran implementation of the method leads to $3\times$ and $7\times$ speedups for $N = 10$ and $N = 100$ respectively, over the current state-of-the-art analytical method (FDCR) also implemented in Fortran. Preliminary results have benchmarked IDSVA in C++

vs. the analytical derivatives in Pinocchio, showing a smaller but still significant $1.6\times$ speedup with a model of ATLAS.

While the proposed FDSVA method is $\mathcal{O}(N^2)$ overall, for practical robotic applications ($N < 100$), the method is dominated by computations that scale with order $\mathcal{O}(Nd)$. The reduction in runtime for partial derivatives enables faster optimization algorithms for both on-line and off-line robotics applications. These improved timings can ultimately lead to better motion planning of legged and industrial robots.

VIII. ACKNOWLEDGEMENT

This work was partially supported by the National Science Foundation EAGER grant CMMI-1835013.

REFERENCES

- [1] M. Neunert et al., "Whole-Body Nonlinear Model Predictive Control Through Contacts for Quadrupeds," in *IEEE Robotics and Automation Letters*, vol. 3, no. 3, pp. 1458-1465, 2018.
- [2] M. Posa, C. Cantu, R. Tedrake, "A direct method for trajectory optimization of rigid bodies through contact," *The International Journal of Robotics Research*, vol. 33, no. 1, pp. 69-81, 2014.
- [3] C. Mastalli, R. Budhiraja, W. Merkt, G. Saurel, B. Hammoud, et al., "Crocodyl: An Efficient and Versatile Framework for Multi-Contact Optimal Control," in *IEEE International Conference on Robotics and Automation (ICRA)*, 2020.
- [4] R. Tedrake and the Drake Development Team, "Drake: Model-based design and verification for robotics" 2019, url - <https://drake.mit.edu>.
- [5] E. Todorov, T. Erez and Y. Tassa, "MuJoCo: A physics engine for model-based control," in *2012 IEEE/RSJ International Conference on Intelligent Robots and Systems*, 2012, pp. 5026-5033.
- [6] J. Carpentier, N. Mansard, "Analytical Derivatives of Rigid-Body Dynamics Algorithms," in *Robotics: Science and Systems (RSS 2018)*, Pittsburgh, United States, Jun. 2018.
- [7] Y. Tassa, T. Erez and E. Todorov, "Synthesis and stabilization of complex behaviors through online trajectory optimization," in *2012 IEEE/RSJ International Conference on Intelligent Robots and Systems*, 2012, pp. 4906-4913.
- [8] J. Koenemann et al., "Whole-body model-predictive control applied to the HRP-2 humanoid," in *2015 IEEE/RSJ International Conference on Intelligent Robots and Systems (IROS)*, 2015, pp. 3346-3351.
- [9] M. Kudruss, P. Manns and C. Kirches, "Efficient derivative evaluation for rigid-body dynamics based on recursive algorithms subject to kinematic and loop constraints," *IEEE Control Systems Letters*, vol. 3, no. 3, pp. 619-624, 2019.
- [10] M. Gifithaler, M. Neunert, M. Stauble, M. Frigerio, C. Semini, and J. Buchli, "Automatic differentiation of rigid-body dynamics for optimal control and estimation," *Advanced Robotics*, vol. 31, no. 22, pp. 1225-1237, 2017.
- [11] J.N. Lyness, and C. B. Moler, "Numerical differentiation of analytic functions," *SIAM Journal on Numerical Analysis*, vol. 4, no.2, pp. 202-210, 1967.
- [12] C. C. Cossette, A. Walsh and J. R. Forbes, "The Complex-Step Derivative Approximation on Matrix Lie Groups," *IEEE Robotics and Automation Letters*, vol. 5, no. 2, pp. 906-913, 2020.
- [13] G. Garofalo, C. Ott and A. Albu-Schaffer, "On the closed form computation of the dynamic matrices and their differentiations," in *2013 IEEE/RSJ International Conference on Intelligent Robots and Systems*, 2013, pp. 2364-2359.
- [14] A. Jain and G. Rodriguez, "Linearization of manipulator dynamics using spatial operators," *IEEE Transactions on Systems, Man, and Cybernetics*, vol. 23, no. 1, pp. 239-248, 1993.

- [15] G. A. Sohl, and J. E. Bobrow, "A recursive multibody dynamics and sensitivity algorithm for branched kinematic chains," *J. Dyn. Sys., Meas., Control*, vol. 123, no. 3, pp. 391-399, 2001.
- [16] R. Featherstone, *Rigid-Body Dynamics Algorithms*, Springer, 2008.
- [17] S. Kuindersma, F. Permenter and R. Tedrake, "An efficiently solvable quadratic program for stabilizing dynamic locomotion," in *2014 IEEE International Conference on Robotics and Automation (ICRA)*, 2014, pp. 2589-2594.
- [18] S. Echeandia and P. Wensing, Numerical methods to compute the coriolis Matrix and christoffel Symbols for rigid-body systems, *ArXiv*, vol. abs/2010.01033, 2020.
- [19] G. D. Niemeyer, "Computational Algorithms for Adaptive Robot Control", Master's thesis, MIT, Boston, 1990.
- [20] G. Niemeyer, J.-J. E. Slotine "Performance in Adaptive Manipulator Control," *The International Journal of Robotics Research*, vol 10, no. 2, pp 149-161, 1991.
- [21] C. L. Lawson, R. J. Hanson, D. R. Kincaid and F. T. Krogh "Basic Linear Algebra Subprograms for Fortran Usage", *ACM Trans. on Math. Softw.*, vol. 5, no. 3, p.- 308-323, Sep. 1979.
- [22] J. Carpentier et al, "The Pinocchio C++ library – A fast and flexible implementation of rigid body dynamics algorithms and their analytical derivatives" in *IEEE International Symposium on System Integrations (SII)*, 2019.

APPENDIX

A. Properties of Spatial Vectors

Assuming $\mathbf{u}, \mathbf{v}, \mathbf{m}, \mathbf{v}_1, \mathbf{v}_2 \in M^6$, and $\mathbf{f} \in F^6$, many spatial vector properties [16] are utilized herein:

- P1. $(\mathbf{v} \times \mathbf{m}) \times = (\mathbf{v} \times)(\mathbf{m} \times) - (\mathbf{m} \times)(\mathbf{v} \times)$
P2. $(\mathbf{v} \times \mathbf{m}) \times^* = (\mathbf{v} \times^*)(\mathbf{m} \times^*) - (\mathbf{m} \times^*)(\mathbf{v} \times^*)$
P3. $(\mathbf{v} \times^* \mathbf{f}) \bar{\times}^* = (\mathbf{v} \times^*)(\mathbf{f} \bar{\times}^*) - (\mathbf{f} \bar{\times}^*)(\mathbf{v} \times)$
P4. $(\mathbf{v}_1 \times \mathbf{v}_2)^T \mathbf{f} = -\mathbf{v}_2^T (\mathbf{v}_1 \times^* \mathbf{f})$
P5. $(\mathbf{v}_1 \times^* \mathbf{f})^T \mathbf{v}_2 = -\mathbf{f}^T (\mathbf{v}_1 \times \mathbf{v}_2)$
P6. $\mathbf{v}_1^T (\mathbf{v}_2 \times^*) \mathbf{f} = \mathbf{f}^T (\mathbf{v}_1 \times \mathbf{v}_2)$
P7. $(\mathbf{u} \times \mathbf{v})^T = -\mathbf{v}^T (\mathbf{u} \times^*)$
P8. $(\mathbf{u} \times^* \mathbf{f})^T = -\mathbf{f}^T \mathbf{u} \times$

B. Main Algorithm

Algorithm 1 IDSVA Algorithm

Require: $\mathbf{q}, \dot{\mathbf{q}}, \ddot{\mathbf{q}}, model$

- 1: $\mathbf{v}_0 = 0; \mathbf{a}_0 = -\mathbf{a}_g$
 - 2: **for** $i = 1$ to N **do**
 - 3: $\mathbf{v}_i = \mathbf{v}_{\lambda(i)} + \phi_i \dot{\mathbf{q}}_i$
 - 4: $\mathbf{a}_i = \mathbf{a}_{\lambda(i)} + \phi_i \ddot{\mathbf{q}}_i + \mathbf{v}_i \times \phi_i \dot{\mathbf{q}}_i$
 - 5: $\dot{\phi}_i = \mathbf{v}_i \times \phi_i$
 - 6: $\ddot{\phi}_i = \mathbf{a}_i \times \phi_i + \mathbf{v}_i \times \dot{\phi}_i$
 - 7: $\mathbf{B}_i^C = \frac{1}{2}[(\mathbf{v}_i \times^*) \mathbf{I}_i - \mathbf{I}_i (\mathbf{v}_i \times) + (\mathbf{I}_i \mathbf{v}_i) \bar{\times}^*]$
 - 8: $\mathbf{f}_i = \mathbf{I}_i \mathbf{a}_i + (\mathbf{v}_i \times^*) \mathbf{I}_i \mathbf{v}_i$
 - 9: **end for**
 - 10: **for** $i = N$ to 1 **do**
 - 11: $\mathbf{t}_1 = \mathbf{I}_i^C \phi_i$
 - 12: $\mathbf{t}_2 = 2(\mathbf{B}_i^C \phi_i + \mathbf{I}_i^C \dot{\phi}_i)$
 - 13: $\mathbf{t}_3 = 2\mathbf{B}_i^C \dot{\phi}_i + \mathbf{I}_i^C \ddot{\phi}_i + \phi_i \times^* \mathbf{f}_i^C$
 - 14: $\mathbf{t}_4 = 2[\mathbf{B}_i^C]^\top \phi_i$
 - 15: $j = i$
 - 16: **while** $j > 0$ **do**
 - 17: $\frac{\partial \tau_j}{\partial q_i} = \phi_j^\top \mathbf{t}_3$
 - 18: $\frac{\partial \tau_i}{\partial q_j} = \ddot{\phi}_j^\top \mathbf{t}_1 + \dot{\phi}_j^\top \mathbf{t}_4$
 - 19: $\frac{\partial \tau_j}{\partial q_i} = \phi_j^\top \mathbf{t}_2$
 - 20: $\frac{\partial \tau_i}{\partial q_j} = 2\dot{\phi}_j^\top \mathbf{t}_1 + \phi_j^\top \mathbf{t}_4$
 - 21: $j = \lambda(j)$
 - 22: **end while**
 - 23: **if** $\lambda(i) > 0$ **then**
 - 24: $\mathbf{I}_{\lambda(i)}^C = \mathbf{I}_{\lambda(i)}^C + \mathbf{I}_i^C; \mathbf{B}_{\lambda(i)}^C = \mathbf{B}_{\lambda(i)}^C + \mathbf{B}_i^C$
 - 25: $\mathbf{f}_{\lambda(i)}^C = \mathbf{f}_{\lambda(i)}^C + \mathbf{f}_i^C$
 - 26: **end if**
 - 27: **end for**
 - 28: **return** $\frac{\partial \tau}{\partial \mathbf{q}}, \frac{\partial \tau}{\partial \dot{\mathbf{q}}}$
-